

# Electric force microscopy of dielectric heterogeneous polymer blends

A.V. Krayev<sup>a</sup>, R.V. Talroze<sup>b,\*</sup>

<sup>a</sup>Quantum Polymer Technologies Corp., 3573 Westwind Blvd, Santa Rosa, CA, USA

<sup>b</sup>Department of Chemical Engineering and Materials Science, University of California Davis, One Shields Avenue, Davis, CA 95616, USA

Received 18 July 2004; received in revised form 24 September 2004; accepted 24 September 2004

Available online 12 October 2004

## Abstract

We report the applicability of Electric Force Microscopy (EFM) for the analysis of thin films of dielectric heterogeneous polymer blends constituted of polymers with both close and significantly different dielectric constants and offer a simple model that enables quantitative analysis of EFM images of such blends.

© 2004 Elsevier Ltd. All rights reserved.

*Keywords:* Polymer blends; Electric force microscopy; EFM

## 1. Introduction

In modern technology polymers are very rarely used as pure components—the final products are usually complex mixtures of polymers and numerous additives such as stabilizers, microparticles, dyes etc. The general trend in modern industry for miniaturization and transition from micro- to nano-level requires the reduction in size of particulate additives and structural units in polymer materials. As a consequence, the analysis of such systems becomes very challenging. To a great extent this challenge has been met with the introduction of scanning probe microscopy (SPM) that has become a powerful method for micron-to-nanometer-scale analysis of different systems including polymers [1]. Topography and topography phase imaging in tapping mode are the most common SPM techniques for investigation of polymers and their composites [2–4]. Electric force microscopy (EFM) is usually applied to the study of conducting materials, especially semiconductors, or composite materials containing conducting fillers [5–7]. To the best of our knowledge there is no information available on the use of EFM for the analysis of dielectric systems.

The main objective of this research is to demonstrate that

EFM may work not only for conductive systems, but also for heterogeneous dielectrics, even if the difference in the dielectric constants of components is small. In this paper, we present the data of the EFM analysis of the structure of dielectric heterogeneous blends composed of polymers with different dielectric constants. We used blends of atactic polypropylene (APP) with poly(*n*-octyl methacrylate) (POMA) and poly(*N,N*-dimethylaminoethyl methacrylate) (PDMAEMA) as a model system. The choice of these polymers was dictated by the following reasons: (i) the components are immiscible and therefore form stable heterogeneous blends; (ii) the values of dielectric constants of these polymers (2.2, 2.8–2.9, and  $\sim 5$  for APP [8], POMA [9] and PDMAEMA, respectively) allow for the EFM investigation of components in heterogeneous blends with both close and significantly different values of dielectric constants. The content of one of the component did not exceed 2–5 wt% in order to have separate inclusions of this minor component which makes the interpretation of SPM images most direct.

## 2. Experimental

### 2.1. Materials

Atactic polypropylene (CAT#23968, LOT#521210) was supplied by Polysciences Inc., POMA ( $M_w \approx 100,000$ ) and

\* Corresponding author.

E-mail address: [rvtalroze@ucdavis.edu](mailto:rvtalroze@ucdavis.edu) (R.V. Talroze).

PDMAEMA (CAT#887, LOT#02) were purchased from SP<sup>2</sup> Scientific Polymer Products Inc. and were used without any further purification. Since we did not find the data on the dielectric constant of PDMAEMA in literature, we estimated it to be equal to the dielectric constant of the corresponding monomer ( $\epsilon_{\text{monomer}} \approx 5$ ) which was obtained from the capacitance measurements of an air gap capacitor filled with monomer at frequencies 1–10 kHz.

## 2.2. Film preparation

For each pair APP-PDMAEMA and APP-POMA 4–6  $\mu\text{m}$  thick films were prepared by casting the 2% solution of chosen polymers in a non-selective solvent (toluene for APP-PDMAEMA, and heptane for APP-POMA) on the surface of a gold-coated glass slide  $12.5 \times 25$  mm. The films of APP-PDMAEMA contained 2, 5 and 98 wt% of PDMAEMA, while APP-POMA films contained 2 and 98 wt% of POMA. Solvent was evaporated at room temperature. The SPM measurements started 15 min after the samples weight became stable.

## 2.3. SPM measurements

SPM measurements were carried out with MT-NDT built Solver-P47-Smena double scan system. We could choose from scanning by probe or scanning by sample option depending on the desired scan size and resolution. For each sample topography and topography phase measurements in tapping mode were taken first with amplitude of cantilever vibration about 30 nm. After that the AC EFM measurements were performed using regular two pass technique when in the first pass the topography was recorded and stored in memory and in the second pass the cantilever was lifted up 30–50 nm over the surface, voltage of 10 V was applied between the cantilever and the golden substrate of the polymer film, and the phase deviation of cantilever oscillation was recorded as it scanned the surface maintaining the preset elevation.

## 3. Results and discussion

### 3.1. APP-PDMAEMA films

A very poor miscibility of APP and PDMAEMA resulted in the segregation of micrometer-scale inclusions of PDMAEMA in the matrix of APP. These inclusions are seen as bright round spots in the topography image (Fig. 1(a)). The bright coloration of these regions means that they are somewhat elevated over the adjacent APP matrix. Topography phase image of the same area (Fig. 1(b)) provides even better contrast. In the topography phase mode the settings of the device were chosen such that the decrease in the phase shift (darker color) corresponded to a stronger repulsion. For that reason the PDMAEMA inclusions in Fig.

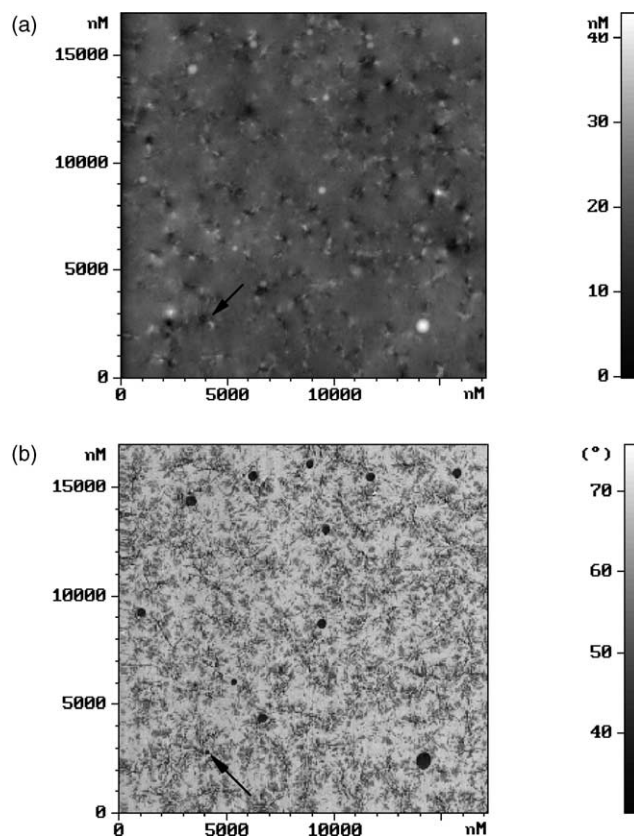


Fig. 1. Topography (a) and topography phase (b) images of 4  $\mu\text{m}$  film of 98%APP+2%PDMAEMA mixture.

1(b) are seen as dark regions because this polymer is more rigid at room temperature, and it is less sticky than APP. The size and location of the bright round regions in Fig. 1(a) coincide with those of dark regions in Fig. 1(b), which means that the corresponding features in the topography and phase images represent PDMAEMA embedded into APP matrix.

Results of EFM measurements of the same area are represented in Fig. 2. Because the dielectric constant of PDMAEMA ( $\epsilon \approx 5$ ) is significantly higher than that of APP

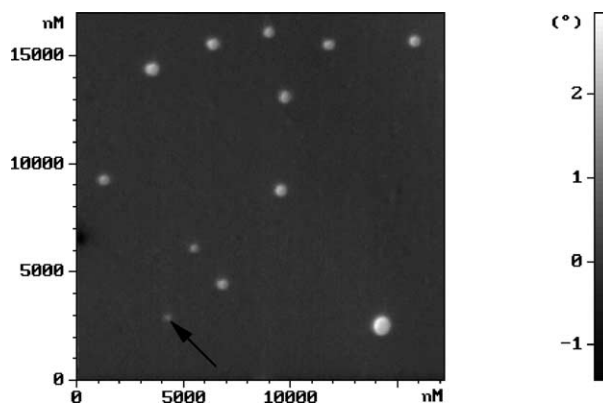


Fig. 2. EFM image of the same area as in Fig. 1. In the second pass the cantilever oscillation phase shift was recorded while cantilever glided 45 nm over the surface and DC voltage of 10 V was applied.

(2.2), the cantilever tip is attracted stronger to the inclusions of PDMAEMA, thereby generating a brighter color in the EFM phase shift image. As we can see, the size and the distribution of bright spots in EFM image correlate with the size and the distribution of the corresponding features in topography and topography phase images. Among these three methods EFM provides the best contrast of the features, especially those with a very small size. For example, one can consider the PDMAEMA inclusion marked by the black arrow. It is practically impossible to find it in the topography image (it is obscured by the adjacent spherulite) and it is very easy to miss this inclusion in the topography phase image due to its small size, but it is very clearly seen in the EFM mode.

In order to make sure that the assignment of bright spots in the EFM images to the inclusions of PDMAEMA is correct, we have investigated films of the above blend containing different amounts of PDMAEMA. The EFM images of APP-PDMAEMA films containing 5 and 98 wt% of PDMAEMA are presented in Fig. 3. The increase in the content of PDMAEMA from 2 to 5% results in the 2–3 fold increase of the diameter of its inclusions (bright spots, Fig. 3(a)). The change in the APP-PDMAEMA blend composition from 98:2 to 2:98 leads to the reversal of the EFM contrast (Fig. 3(b)) compared to the data given in Fig. 2, because the APP inclusions in PDMAEMA matrix have the lower dielectric constant.

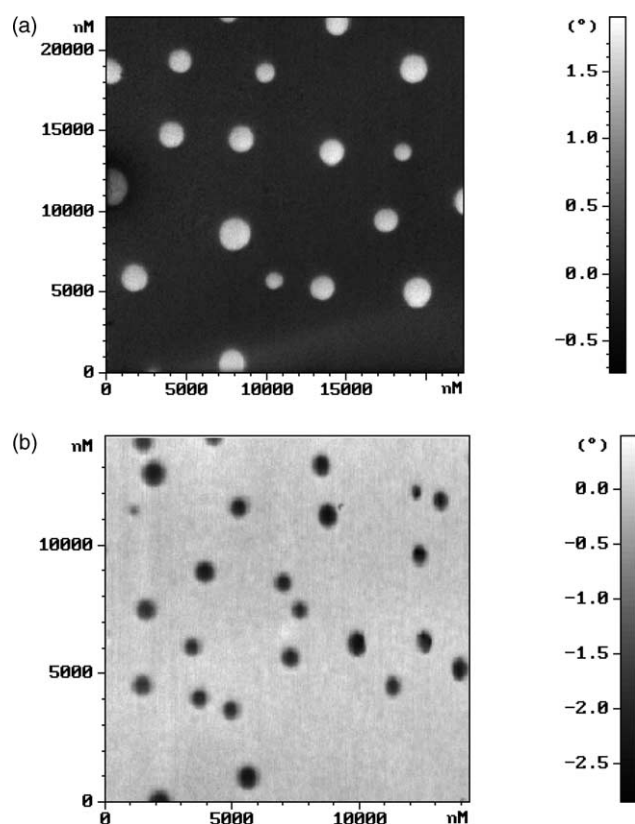


Fig. 3. EFM images of APP-PDMAEMA films with the PDMAEMA content of 5% (a) and 98% (b).

It is important to understand how the contrast of SPM images of a heterogeneous polymer blend depends on the distribution of inclusions across the thickness of the film. For that purpose we modified a sample of an APP-PDMAEMA film originally cast from toluene solution by adding  $\sim 0.1$  ml of heptane on top of it. Heptane dissolved the APP matrix but not PDMAEMA inclusions, because of the negligible solubility of the latter in this solvent (it is important to stress that NO polymer was removed from the sample!). After heptane evaporated, the distribution of PDMAEMA inclusions across the thickness of the film changed dramatically in comparison with the original one, though the overall composition of the blend remained the same. The topography and topography phase images of this modified film show no polymer phase separation at the surface (Fig. 4). Contrary to the above images, the EFM image has several features (Fig. 5(b)), though the contrast is much fainter than in case of inclusions of PDMAEMA coming to the surface (Figs. 2 and 3(a)).

### 3.2. APP-POMA films

The dielectric constants of APP ( $\epsilon=2.2$ ) and PDMAEMA ( $\epsilon \approx 5$ ) are significantly different. It was interesting though to investigate the sensitivity of EFM for analysis of heterogeneous systems with close values of

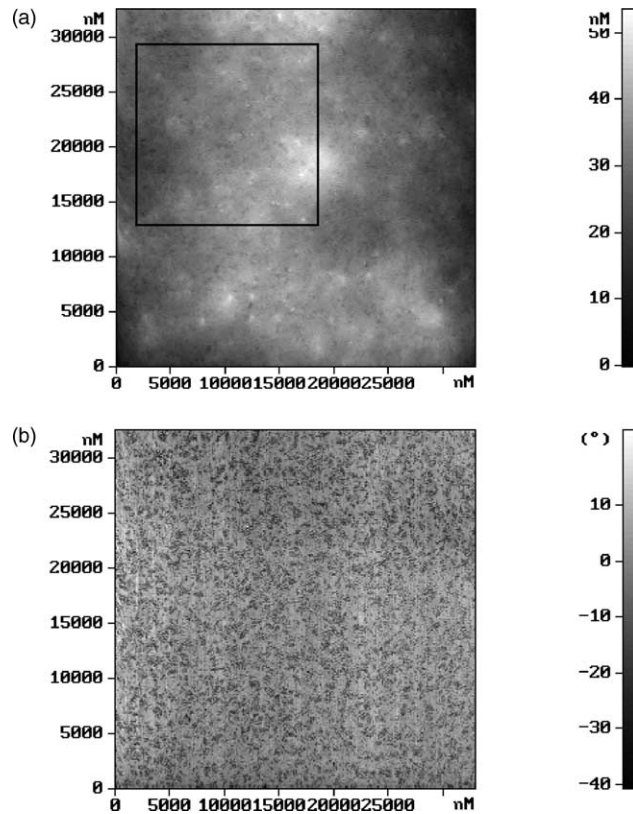


Fig. 4. Topography (a) and topography phase (b) image of the 98%APP + 2%PDMAEMA film modified by dissolution in heptane. The area inside the square was investigated in EFM mode (Fig. 5).

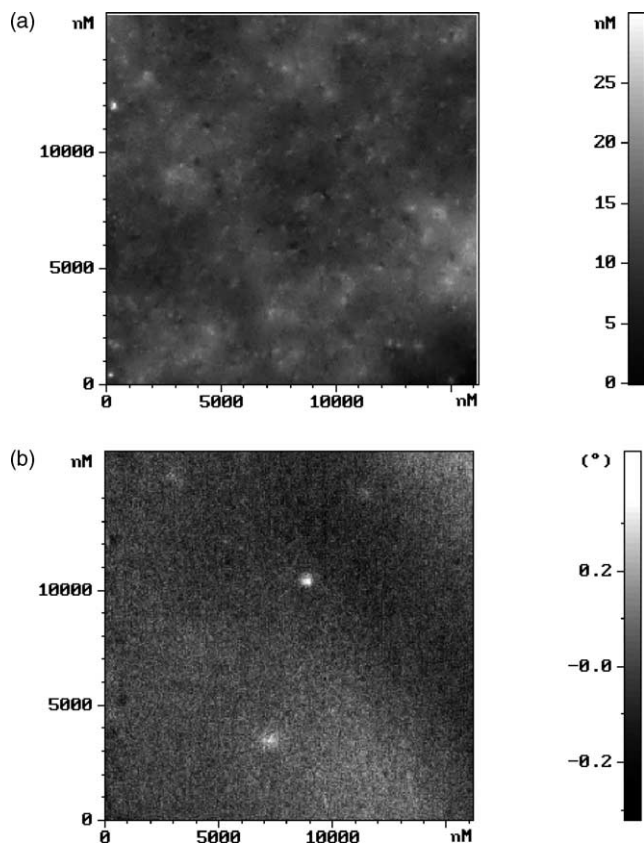


Fig. 5. Two pass EFM images of the area within the square in Fig. 4a. (a)—topography image taken in the first pass, (b)—EFM phase shift image.

dielectric constants of constituent components. The blend of APP and poly(*n*-octyl methacrylate) (POMA) serves this purpose perfectly. These two polymers have close values of dielectric constant ( $\epsilon=2.2$  for APP and  $\epsilon=2.8$ – $2.9$  for POMA) and have readily available common solvents—heptane and toluene.

The topography and topography phase images of the APP-POMA film obtained in the tapping mode are presented in Fig. 6, whereas EFM image of the same spot is shown in Fig. 7. From Fig. 7 one can see that the inclusions of POMA in APP are well-defined in the EFM image. Moreover, as it was for APP-PDMAEMA films, EFM provides the highest contrast as even the small size inclusions, which are hard to find in topography or topography phase images, can be resolved in the EFM mode.

The change of APP-POMA composition from 98:2 to 2:98 results in reversal of the contrast of the EFM pictures of the latter blend (Fig. 8) for the same reason it happened in case of the APP-PDMAEMA compositions.

### 3.3. Quantitative model of EFM of dielectric films

In EFM the attractive force between the cantilever and the sample is given by general formula

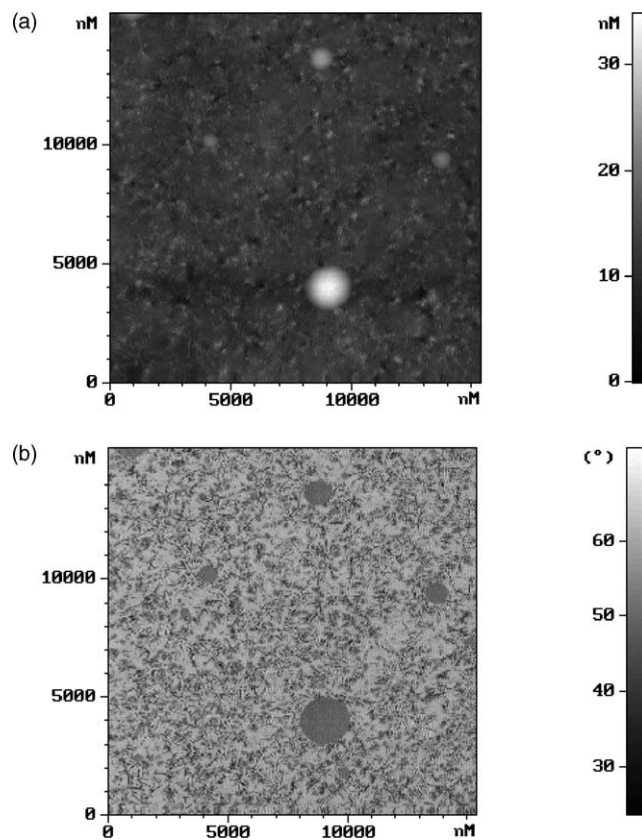


Fig. 6. Topography (a) and topography phase images (b) of 5  $\mu\text{m}$  film of 98% APP+2% POMA blend.

$$F = -\frac{U^2 \partial C / \partial z}{2} \quad (1)$$

where  $U$  is the voltage between the sample and the cantilever and  $C$  is cantilever-to-sample capacitance. The approach where the cantilever-to-sample capacitance is calculated using a plane capacitor approximation, is usually correct for EFM of conducting samples. However, it cannot be applied to the thick (thickness is much bigger than both the cantilever-to surface distance and the tip radius) dielectric films. In a plane capacitor the distance between the electrodes  $d$  must be significantly less than the linear

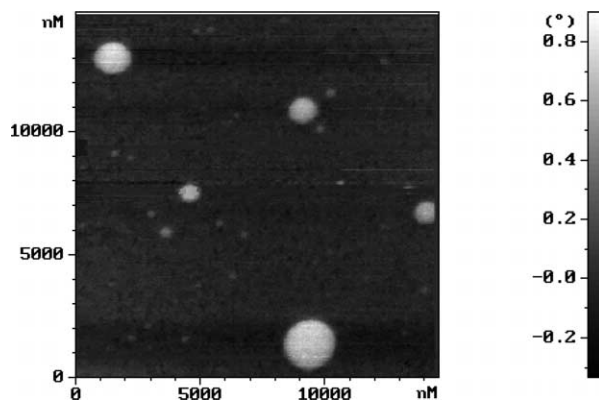


Fig. 7. EFM image of the same area as in Fig. 6.

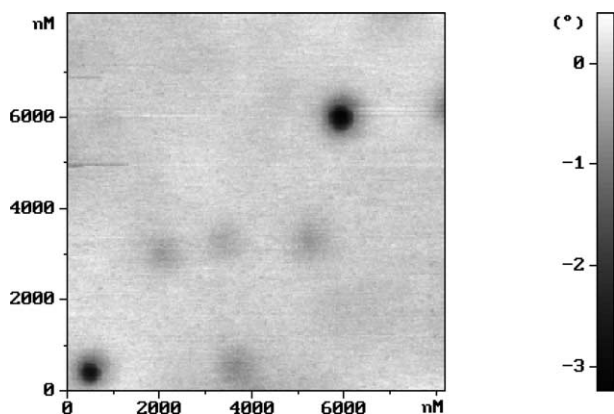


Fig. 8. EFM image of APP-POMA blend having 98% of POMA. The contrast is reversed in comparison with the image in Fig. 7.

size (width) of these electrodes  $r$ , i.e.  $d \ll r$ . In case of EFM of micrometer-thick dielectric films the ratio of these parameters is reversed:  $d \gg r$ , and therefore the plane capacitor approach is inapplicable.

In order to estimate how the attractive force depends on the distance between the tip and the surface, and the tip curvature radius, one can approximate the cantilever tip with a sphere of the same radius [10]. The calculation of the three-dimensional case of the sphere over the metal surface may be reduced down to one-dimensional case by using the method of electrostatic reflections. The attractive force calculated by this method is given by the following formula:

$$F = \frac{U^2}{4} \frac{r^2}{(Z - r)^2} \quad (2)$$

where  $r$  is the sphere (cantilever) radius and  $Z$  is the distance between the sphere's center and the metal surface. The application of the method of electrostatic reflections for a sphere over the layer of dielectric placed atop of conducting surface creates unnecessary complexity because of the presence of two interfaces. In order to keep the calculations simple, one can make a further approximation and replace the model of a sphere over the plane by the model of a spherical capacitor with the internal radius  $r$  and the external radius  $Z$ . This model also gives an adequate description of the attractive force as a function of the distance and the curvature radius. It is seen from the comparison of the expression (2) with the expression of the attractive force for the case of spherical capacitor where no dielectric layer is involved (formula (3))

$$F = \frac{U^2}{2} \frac{r^2}{(Z - r)^2} \quad (3)$$

Formula (3) differs from (2) only by factor 2 which is insignificant for our consideration.

The main advantage of the spherical capacitor approach is that it gives a fairly simple expression of the attractive force in case when there is a dielectric layer (Fig. 9(a)) of thickness  $d$  and dielectric constant  $\epsilon$  inside the capacitor

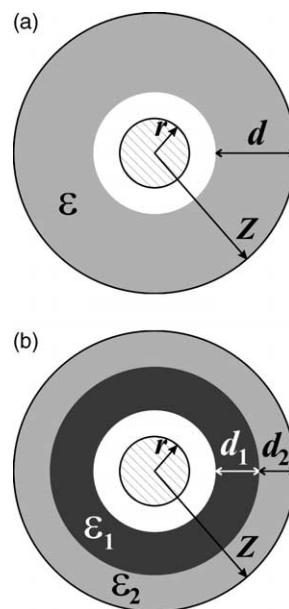


Fig. 9. Model of a spherical capacitor with one (a) and two (b) layers of dielectric.

(formula (4)):

$$F = \frac{U^2}{2} \frac{r^2 \epsilon (Z^2 (\epsilon - 1) + (Z - d)^2)}{(Z \epsilon (Z - d - r) + dr)^2} \quad (4)$$

Typically, the distance between the tip and the surface  $Z - d - r$  is about 20–50 nm, which is approximately the same as the curvature radius  $r$  of a tip with a conducting layer on it (20–40 nm). This means that during EFM measurements of several micrometers thick films the thickness  $d$  is much bigger than both the curvature radius of the cantilever's tip and the distance between the cantilever tip and the surface  $Z - d - r$ , i.e.  $d \sim Z \gg r \sim (Z - d - r)$ . Taking this into account, formula (4) may be transformed into (5):

$$F = \frac{U^2}{2} \frac{\epsilon (\epsilon - 1)}{(\epsilon + 1)^2} \quad (5)$$

In AC EFM that was used in our experiments the change of phase shift  $\Delta\Theta$  is proportional to the attractive force gradient. From differentiation of (4) one can get under the familiar assumption of  $d \sim Z \gg r \sim (Z - d - r)$

$$\Delta\Theta \sim \frac{\partial F}{\partial Z} \approx - \frac{U^2}{2} \frac{\epsilon^2 (\epsilon - 1)}{r (\epsilon + 1)^3} \quad (6)$$

The graphs of  $\epsilon(\epsilon - 1)/(\epsilon + 1)^2$  and  $\epsilon^2(\epsilon - 1)/(\epsilon + 1)^3$  as a function of dielectric constant value are given in Fig. 10. The curves are steep at low dielectric constants but attain the plateau at  $\epsilon > 20$ . In general, these curves reflect the sensitivity of the EFM method to dielectric constant of the material and may be used for quantitative estimation of the value of dielectric constants of the constituents of a heterogeneous system. The EFM contrast of two adjacent regions of the film having a similar geometrical parameters and a given difference of dielectric constants will be

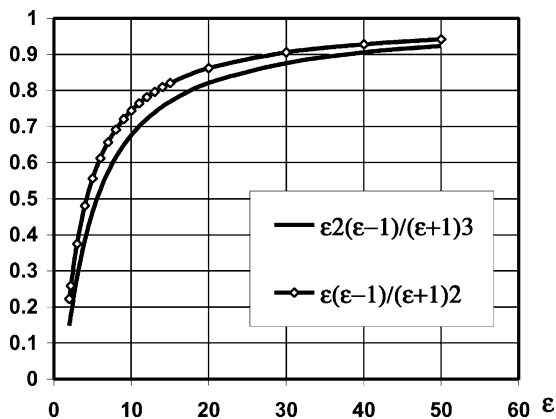


Fig. 10. Plots of  $\varepsilon(\varepsilon-1)/(\varepsilon+1)^2$  (hollow diamonds) and  $\varepsilon^2(\varepsilon-1)/(\varepsilon+1)^3$  as a function of the value of a dielectric constant.

maximal if the absolute values of dielectric constants are low.

It is fairly simple to show that the expression for the attractive force in the model of a spherical capacitor when there are two layers of different dielectrics on top of each other (Fig. 9(b)) may be reduced down to formula (7) if  $Z \sim d_1 \sim d_2 \gg (Z - d_1 - d_2) \sim r$ .

$$F = \frac{U^2}{2} \frac{r^2 \varepsilon_1 Z^2 (\varepsilon_1 - 1) (Z - d_2)^2}{(\varepsilon_1 (Z - d_1 - d_2 - r) (Z - d_2) + d_1 r)^2} \quad (7)$$

As it is seen from formula (7), the attractive force is defined only by the dielectric layer coming to the free surface, provided the assumptions  $Z \sim d_1 \sim d_2 \gg (Z - d_1 - d_2) \sim r$  are correct. It explains relatively poor EFM contrast for the APP-PDMAEMA film represented in Fig. 5(b), where inclusions of PDMAEMA were located under the surface of the APP film.

#### 4. Conclusions

It has been shown that EFM may be a convenient method for the investigation of heterophase polymer systems composed of polymers with different dielectric constants. A simple mathematical model shows that EFM is particularly sensitive when the value of the dielectric constant of one of the components is low. EFM may provide more accurate information than topography or topography phase images about the distribution of the phases along the surface of a heterogeneous film and inside the film in the vicinity of the surface.

#### Acknowledgements

Authors are grateful to Dr Leonid Grigorov and Dr Eugene Zubarev for helpful discussions.

#### References

- [1] Magonov SN. AFM in analysis of polymer. In: Meyers RA, editor. Encyclopedia of analytical chemistry. Chichester: Wiley; 2000. p. 7432–91.
- [2] Raghavan D, Gu X, Nguyen T, VanLandingham M, Karim A. Macromolecules 2000;33:2573–83.
- [3] Cabral JT, Higgins JS, Yerina NA, Magonov SN. Macromolecules 2002;35:1941–50.
- [4] Petrovic ZS, et al. Polymer 2004;45(12):4285–95.
- [5] Lei CH, Das A, Elliott M, Macdonald JE. Appl Phys Lett 2003;83(3): 482–4.
- [6] Bachtold A, Fuhrer MS, Plyasunov S, Forero M, Anderson EH, Zettl A, McEuen PL. Phys Rev Lett 2000;84(26):6082–5.
- [7] Viswanathan R, Heany MB. Phys Rev Lett 1995;75(24):4433–6.
- [8] Brosseau C. J Appl Phys 1994;75(1):672–4.
- [9] Kawamura Y, et al. J Polym Sci, Part A-2 1969;7(9):1559–75.
- [10] Sarid D. Scanning force microscopy. Oxford: Oxford University Press; 1991.